CENTRAL RESEARCH LIBRARY
DOCUMENT COLLECTION

OAK RIDGE NATIONAL LABORATORY
operated by
UNION CARBIDE CORPORATION
NUCLEAR DIVISION
for the
U.S. ATOMIC ENERGY COMMISSION

LOCKHEED MARTIN ENERGY RESEARCH LIBRARIES
3 4456 0513748 3

ORNL - TM - 2630
COPY NO. - 314
DATE - June 23, 1969

Neutron Physics Division

CALCULATION OF THE RESIDUAL PHOTON DOSE RATE DUE TO THE ACTIVATION OF CONCRETE BY NEUTRONS FROM A 3-GeV PROTON BEAM IN IRON*

T. W. Armstrong and J. Barish†

Abstract

Calculations have been carried out to determine the time dependence of the residual photon dose rate inside an accelerator tunnel due to a 3-GeV proton beam located on the axis of an iron cylinder. The photon dose rate produced by the activation of the concrete tunnel wall is calculated and combined with the results from a previous calculation for the dose rate contributed by the iron to obtain the total photon dose rate inside the tunnel. The effectiveness of lowering the total photon dose rate by reducing the ^{24}Na production in the concrete is evaluated. The development of the nucleon-meson cascade, the residual nuclei production, and the photon transport are calculated using Monte Carlo methods.

OAK RIDGE NATIONAL LABORATORY
CENTRAL RESEARCH LIBRARY
DOCUMENT COLLECTION
LIBRARY LOAN COPY
DO NOT TRANSFER TO ANOTHER PERSON
If you wish someone else to see this document, send in name with document and the library will arrange a loan.

---

*Submitted for journal publication.

†Computing Technology Center, Union Carbide Corporation, Oak Ridge, Tennessee.

NOTICE This document contains information of a preliminary nature and was prepared primarily for internal use at the Oak Ridge National Laboratory. It is subject to revision or correction and therefore does not represent a final report.

LEGAL NOTICE

This report was prepared as an account of Government sponsored work. Neither the United States, nor the Commission, nor any person acting on behalf of the Commission:

A. Makes any warranty or representation, expressed or implied, with respect to the accuracy, completeness, or usefulness of the information contained in this report, or that the use of any information, apparatus, method, or process disclosed in this report may not infringe privately owned rights; or

B. Assumes any liabilities with respect to the use of, or for damages resulting from the use of any information, apparatus, method, or process disclosed in this report.

As used in the above, "person acting on behalf of the Commission" includes any employee or contractor of the Commission, or employee of such contractor, to the extent that such employee or contractor of the Commission, or employee of such contractor prepares, disseminates, or provides access to, any information pursuant to his employment or contract with the Commission, or his employment with such contractor.

TABLE OF CONTENTS

Page No.

I. Introduction ---------- 4

II. Results ---------- 5

Photon Dose Rate Due to Radionuclides Other Than ^{24}Na Produced in Concrete ---------- 8

Photon Dose Rate Due to ^{24}Na Production in Concrete ---------- 10

Photon Dose Rate Due in Iron ---------- 12

Total Photon Dose Rate ---------- 12

Appendix A ---------- 19

Appendix B ---------- 24

LOCKHEED MARTIN ENERGY RESEARCH LIBRARIES

3 4456 0513748 3

I. INTRODUCTION

Protons that stray from the beam of a high-energy proton accelerator can, as a result of nuclear interactions, produce radioactive residual nuclei in the surrounding materials. The decay of such radionuclides produces a source of photons after shutdown that presents a potential radiation hazard to personnel requiring entry into the accelerator tunnel. Calculations have been carried out to determine the photon dose rate in an accelerator tunnel as a function of time after shutdown due to photons produced in the material immediately surrounding the beam, such as the magnets, and due to photons produced in the concrete enclosure walls. Of particular interest are a) the contribution to the photon dose rate in the tunnel due to the decay of radionuclides produced in the material immediately surrounding the beam relative to the contribution of radionuclides produced in the concrete, b) the contribution of ^{24}Na produced in the concrete relative to other radionuclides produced in the concrete, and c) the ^{24}Na production by low-energy neutron capture relative to other ^{24}Na production modes. The ^{24}Na production due to low-energy neutron capture by the sodium in the concrete can be controlled, at least to some extent, by choosing concrete materials with low sodium content or by adding appropriate materials, such as boron, to the concrete that will reduce the low-energy neutron flux. Thus, if the individual contributions to the total photon dose rate indicated above are known, a decision can be made as to whether it is worthwhile to reduce the ^{24}Na production by neutron capture.

The calculations have been performed for a beam of 3-GeV protons traveling along the axis of an infinitely long cylinder 40 g/cm^2 in radius.[b] It is assumed that the number of protons per unit distance leaving the beam

is constant during irradiation and that these primary protons have their initial interaction on the beam axis without undergoing energy loss. Surrounding the iron is a void that extends to a radius of 7.34 ft, at which point the concrete begins and extends to infinity. The composition of the concrete is taken to be (in weight %): O, 48.99; Ca, 37.10; C, 9.47; Al, 1.32; H, 0.80; Si, 0.39; Fe, 0.54; Mg, 0.39; and Na, 1.00.[c]

The photon dose rate due to photons escaping from the iron has been calculated previously,[1] hereinafter referred to as paper 1. In the present paper, the photon dose rate due to the activity induced in the concrete is calculated and compared with the iron contribution presented in paper 1. As in paper 1, the calculations were carried out using the Monte Carlo programs of Coleman[2] and Irving *et al.*[3] to determine the development of the nucleon-meson cascade and residual nuclei production, and the Monte Carlo program of Trubey and Emmett[4] to obtain the photon transport. The details of the method of calculation are the same as discussed for the 3-GeV beam in paper 1.

II. RESULTS

The neutron, proton, and charged pion fluxes as a function of radial depth in the concrete are given in Fig. 1. The error bars in this and subsequent figures correspond to statistical errors of one standard deviation. In Fig. 2 the neutron flux per unit energy at the surface of the concrete due to all neutrons and due to only those neutrons that have escaped from the iron and entered the concrete is presented. It is evident from these figures that the total (nucleon and charged pion) flux in the concrete is predominantly due to neutrons and that the low-energy ($\lesssim$ a few MeV) portion of the neutron flux in the concrete is due to the high-energy neutrons that

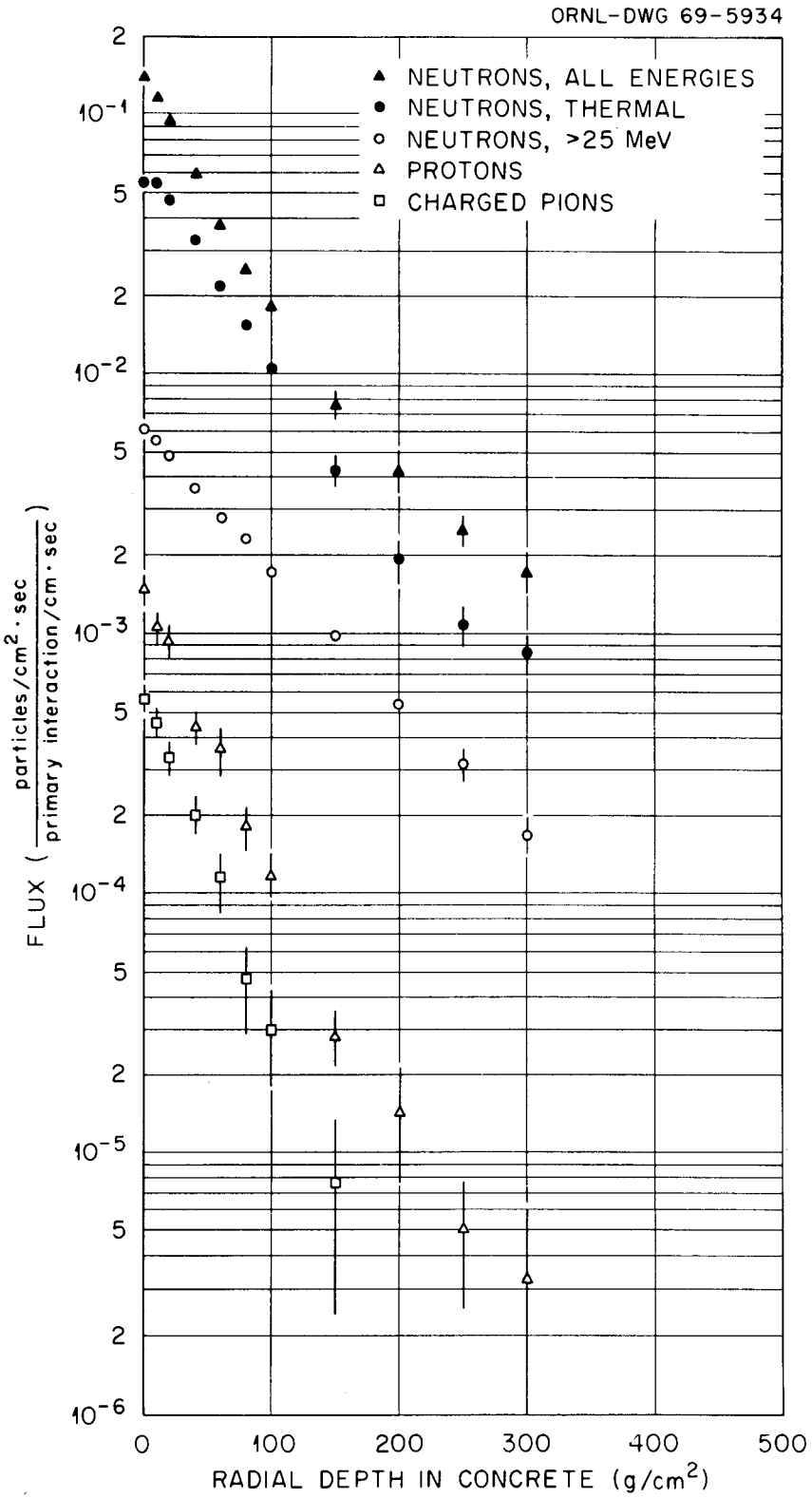

Fig. 1. Particle Fluxes in Concrete.

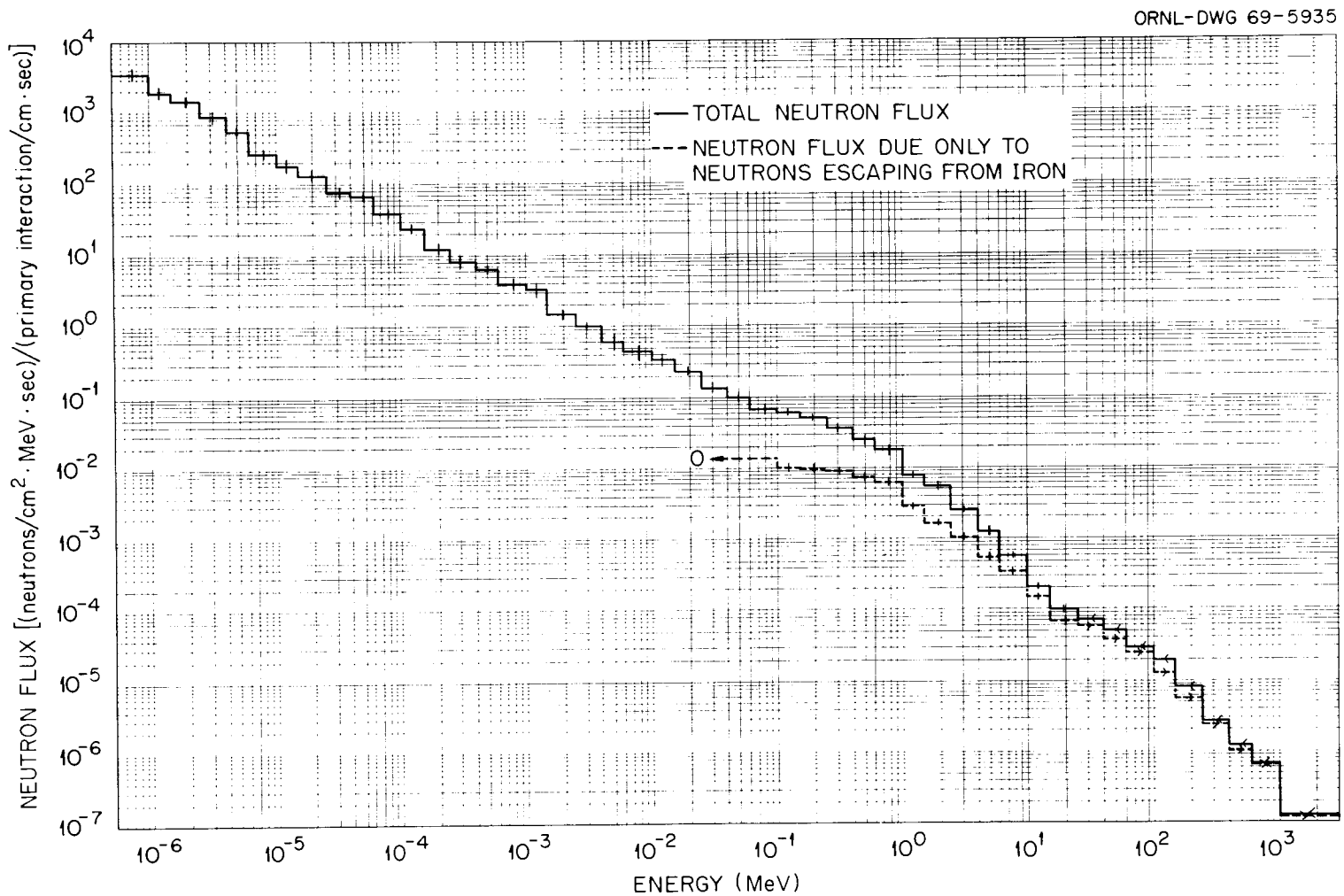

Fig. 2. Neutron Flux Spectra at Tunnel Wall.

enter the concrete rather than the low-energy neutrons that escape from the iron.

In determining the photon dose rate inside the tunnel, the contribution due to radionuclides other than ^{24}Na produced in the concrete, ^{24}Na produced in the concrete, and radionuclide production in the iron will be considered separately.

Photon Dose Rate Due to Radionuclides Other Than ^{24}Na Produced in Concrete

Figure 3 shows the calculated residual-nuclei production rate in the concrete due to particles with energies above 25 MeV. This production rate corresponds to the residual nuclei produced over all radial depths per unit distance along the beam axis per unit time during irradiation. The residual nuclei production is available directly from the Coleman program; that is, explicit values for the production cross sections are not required since they are, in effect, computed in the intranuclear-cascade and evaporation phases of the transport calculation.

The residual-nuclei production in Fig. 3 is seen to be divided into two broad groups according to the residual mass number. The nuclei with $A \gtrsim 20$ are produced primarily from oxygen, and nuclei with $A \gtrsim 20$ are produced primarily from calcium. This dichotomy is, of course, a consequence of the large amounts of oxygen and calcium in the concrete.

Those residual nuclei which are radioactive with half-lives greater than several minutes and which emit photons, either directly in the decay process or by subsequent positron annihilation, are indicated in Fig. 3. The radionuclide production by particles below 25 MeV is negligible except for ^{24}Na production by neutrons. The production of ^{24}Na, both by neutrons below 25 MeV and by particles above 25 MeV, will be discussed later.

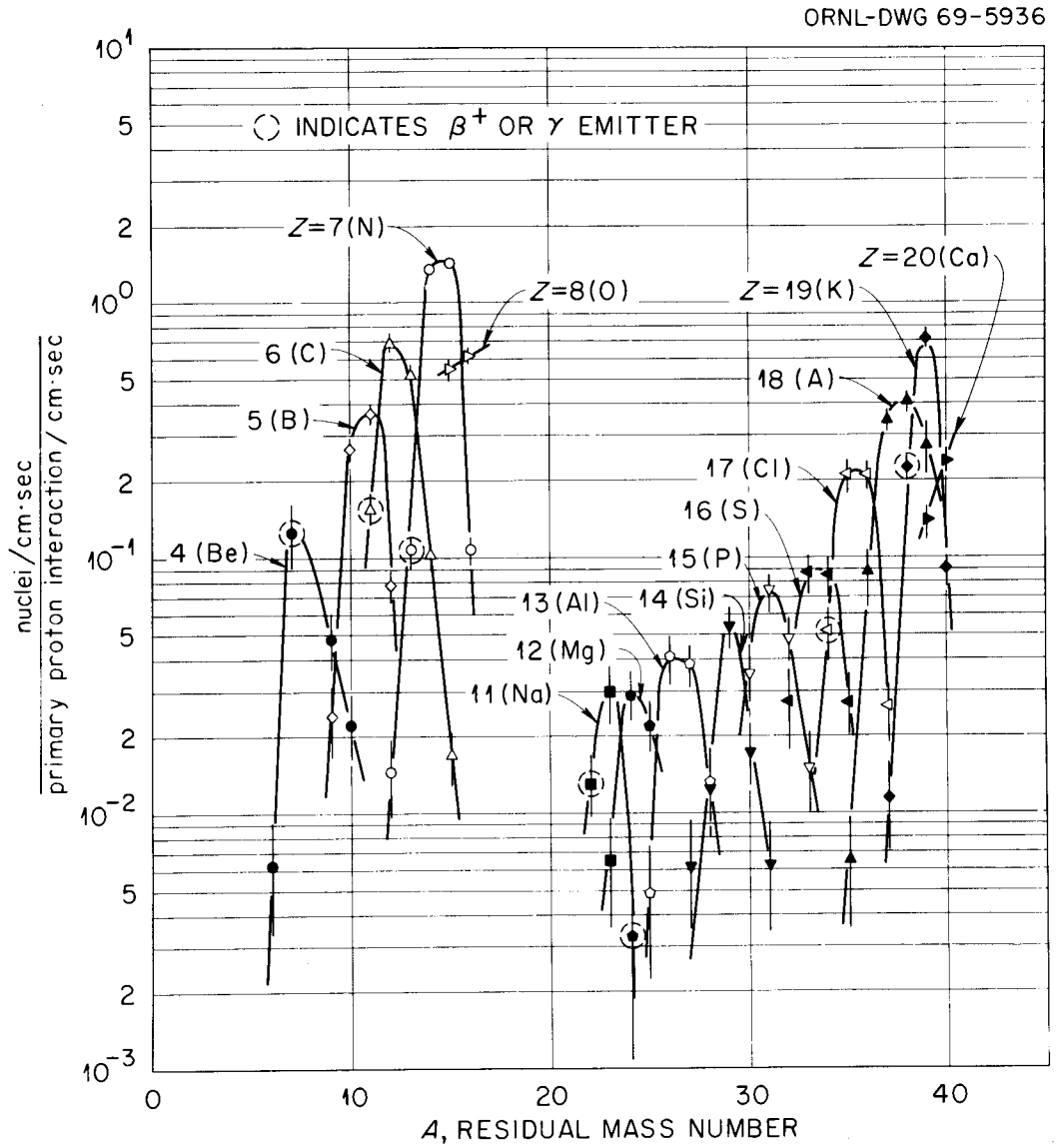

Fig. 3. Residual Nuclei Production in Concrete.

From the spatial distribution of those radionuclides other than ^{24}Na indicated in Fig. 3 (^{7}Be, ^{11}C, ^{13}N, ^{22}Na, ^{34}Cl, and ^{38}K)[d] and from knowledge of the decay modes for these radionuclides, the photon source distribution is defined. This source distribution was then used as input to the photon transport code to obtain the photon flux at the surface of the tunnel wall, and the flux-to-dose factors given in Ref. 5 were then applied to obtain the photon dose rate. The photon dose rate at the tunnel wall due to radionuclides other than ^{24}Na produced over an infinite irradiation time is given in Fig. 4 as a function of time after shutdown.[e]

Photon Dose Rate Due to ^{24}Na Production in Concrete

The method used to determine the ^{24}Na production is somewhat different from that described above for the production of other radionuclides in the concrete. As indicated in Fig. 3, the statistics on the ^{24}Na production by particles above 25 MeV are poor, even when the production is summed over all radial depths. However, adequate statistics for the ^{24}Na production can be obtained by performing an energy integration of the product of the spatially dependent particle spectra, which are available from the transport programs, and the cross sections for each production mode. This alternate method was used to obtain the ^{24}Na production both above and below 25 MeV. The disadvantage of this method is that cross sections are required for each production mode, and some of the needed cross sections are not well known.

The production of ^{24}Na from Ca, Si, Al, Mg, and ^{23}Na was considered. The only production mode not included was the production from Fe; however, this contribution is expected to be negligible because of the low Fe content of the concrete and because the production cross section is expected to be

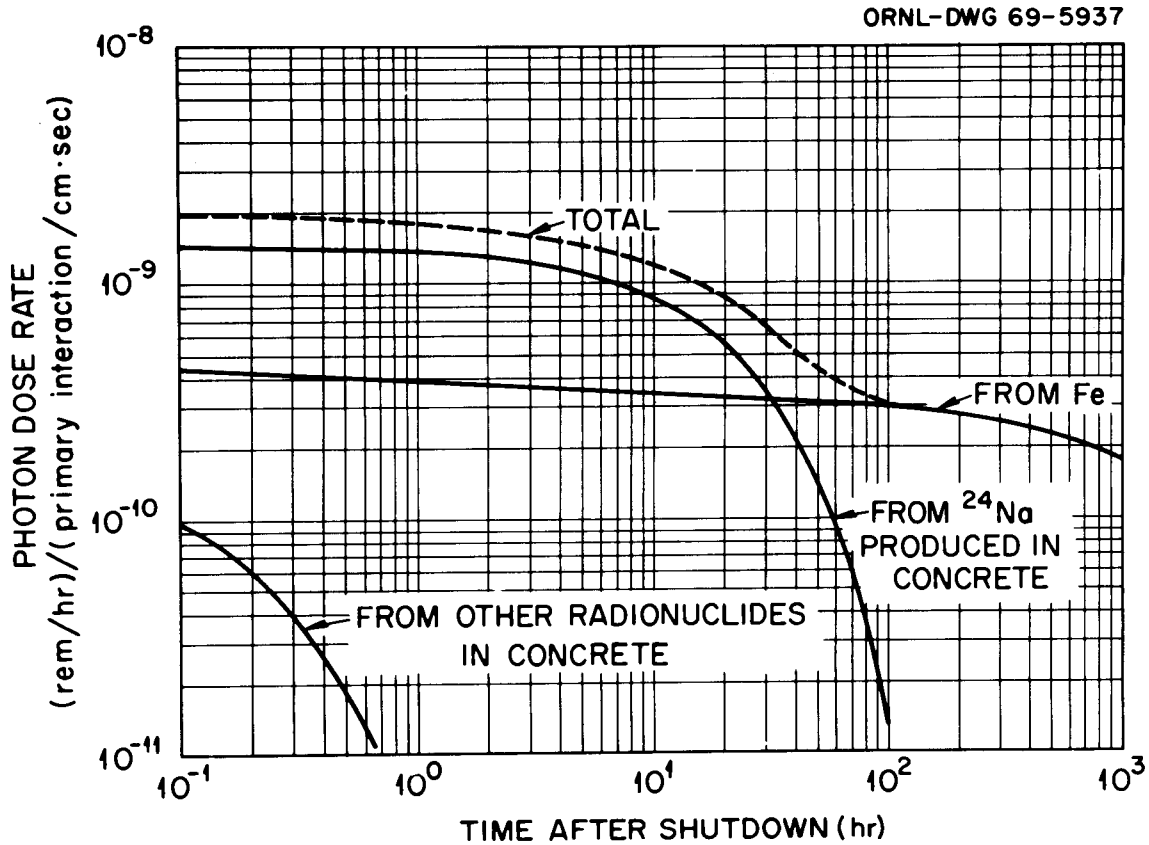

Fig. 4. Photon Dose Rate at Surface of Tunnel Wall After Infinite Irradiation Time for Concrete with 1% Sodium by Weight.

small. Experimental cross sections were used where available and were supplemented by cross sections from the intranuclear-cascade calculations of Bertini[6] and by the empirical formula of Rudstam.[7] Still, some interpolation and extrapolation were required to obtain the cross sections needed to carry out the calculations. Although some rather crude approximations were necessary, the approximations used are not crucial since, as will be shown below, the ^{24}Na production is dominated by the ^{23}Na(n,γ)^{24}Na mode, and this cross section is rather well known. The production cross sections used are given in Appendix A.

In Fig. 5 the ^{24}Na production by various modes is given as a function of radial depth in the concrete. It is evident that the dominant ^{24}Na production mode is low-energy neutron capture by ^{23}Na. The photon dose rate at the tunnel wall due to ^{24}Na is shown in Fig. 4 as a function of time after shutdown.

Photon Dose Rate Due to Iron

The photon dose rate at the surface of the iron cylinder due to radionuclide production in the iron is available from paper 1. To obtain the dose rate as a function of radius in the tunnel, a geometric attenuation factor inversely proportional to the radius was applied to the dose rate at the surface of the iron cylinder.[f] The photon dose rate at the tunnel wall due to photons escaping from the iron is given in Fig. 4 as a function of time after shutdown.

Total Photon Dose Rate

The total photon dose rate, that is, the sum of the contributions due to the radionuclides produced in the iron, the ^{24}Na produced in the concrete, and radionuclides other than ^{24}Na produced in the concrete, at the surface

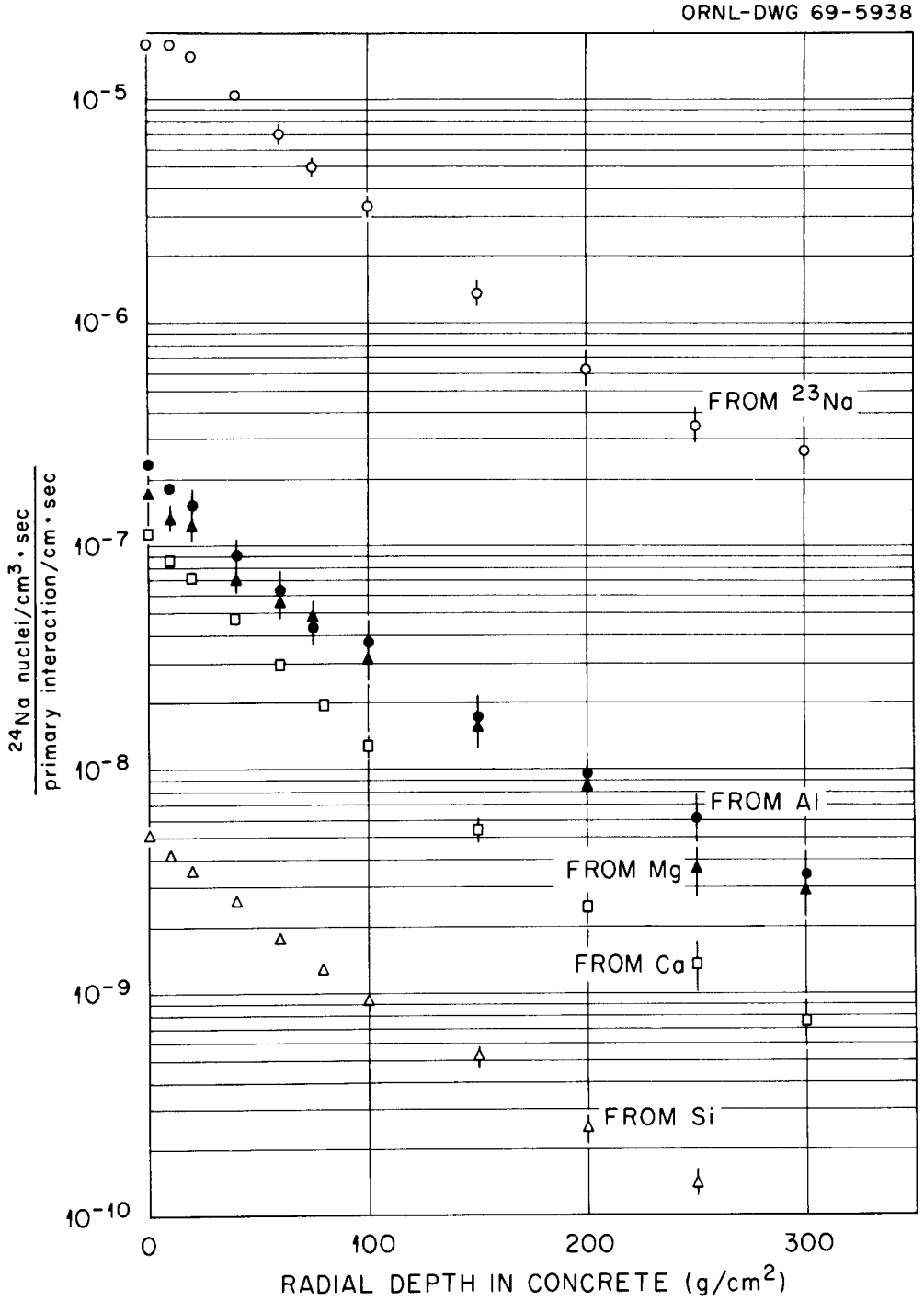

Fig. 5. ^{24}Na Production in Concrete for Various Production Modes.

of the tunnel wall is shown in Fig. 4 as a function of shutdown time. The concrete contribution is dominated by ^{24}Na, which, as discussed earlier, is due almost entirely to low-energy neutron capture by the sodium in the concrete. Thus, by reducing the sodium content of the concrete and/or by reducing the low-energy neutron flux, it is possible to lower the total photon dose rate at the tunnel wall by a factor of ~ 4.5 for shutdown times less than several hours. For shutdown times that are long compared to the 15-hour half-life of ^{24}Na, the total dose rate is dominated by the photons from the ^{54}Mn induced in the iron, which has a half-life of 300 days.

The relative contribution of the iron and concrete to the total photon dose rate at points inside the tunnel is not the same as that at the tunnel wall. This is because the dose rate due to the iron is inversely proportional to the distance from the beam axis, whereas it can be shown (see Appendix B) that the dose rate due to the concrete is constant inside the tunnel and equal to the dose rate at the tunnel wall.[g] From the results given in Fig. 4, the total photon dose rate at points inside the tunnel can be constructed (see Figs. 6 and 7). Thus, the effectiveness of reducing the total dose rate by lowering the concrete contribution depends on the distance from the beam axis as well as the time after shutdown. A measure of this effectiveness is given by the ratio of the total dose rate to the dose rate from the iron since, if the concrete contribution is eliminated, the total dose rate is reduced by a factor equal to this ratio. In Fig. 8 this ratio is given at points inside the tunnel for various shutdown times.[h] Thus, although the elimination of the concrete contribution would, for shutdown times less than several hours, lower the total photon dose rate at the tunnel wall by a factor of ~ 4.5, the reduction at points approximately

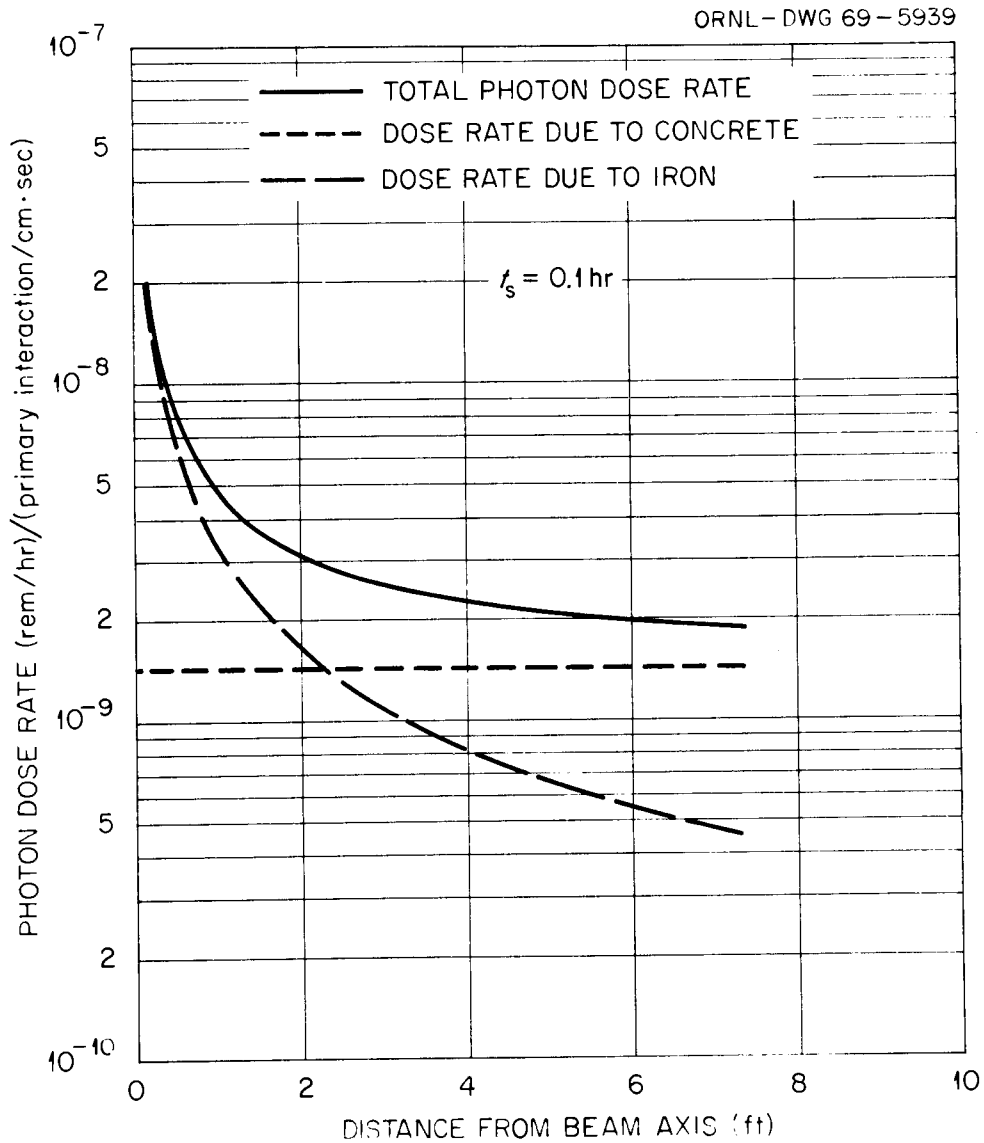

Fig. 6. Photon Dose Rate Inside the Tunnel for a Shutdown Time of 0.1 Hour.

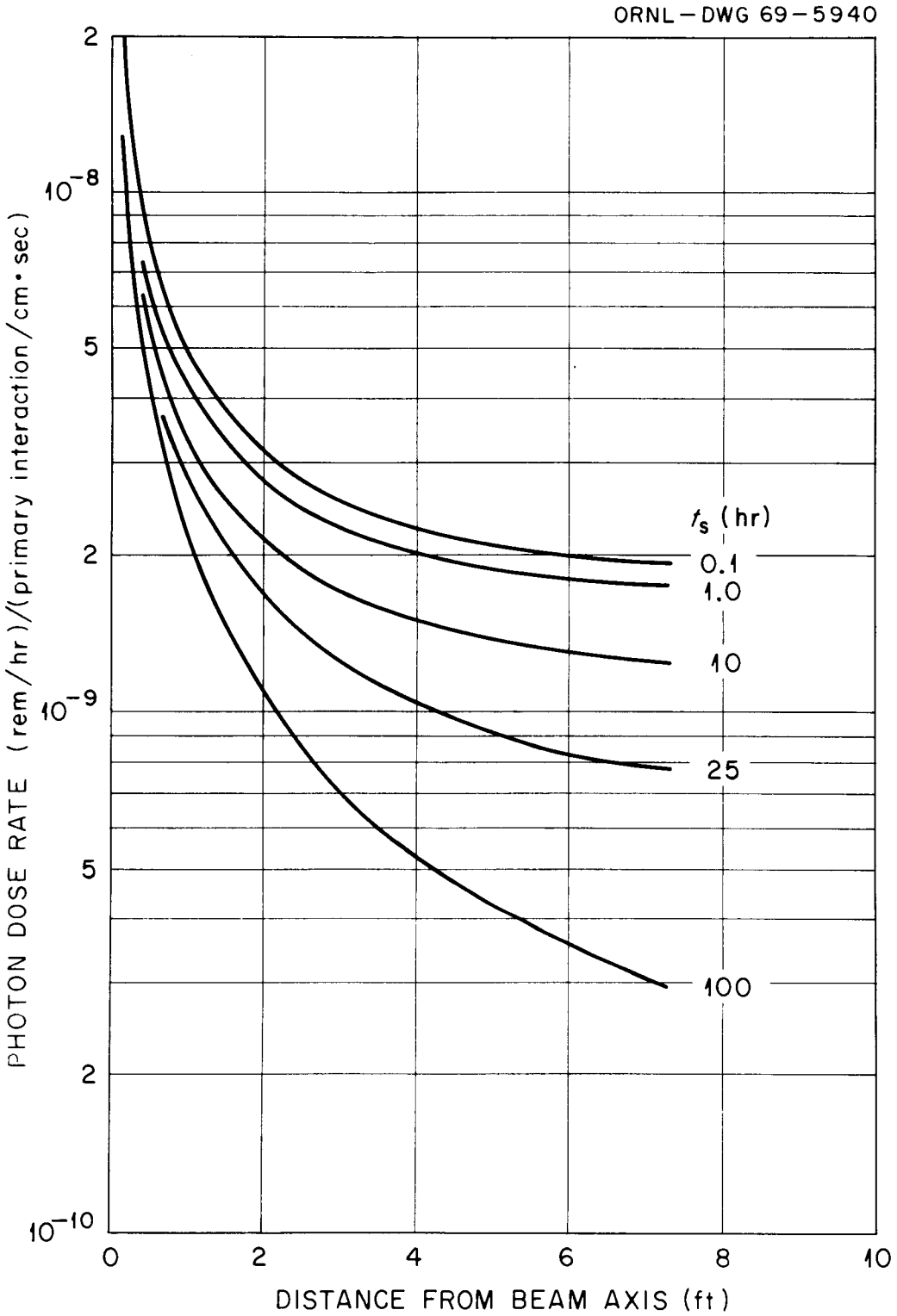

Fig. 7. Total Photon Dose Rate Inside the Tunnel for Various Shutdown Times.

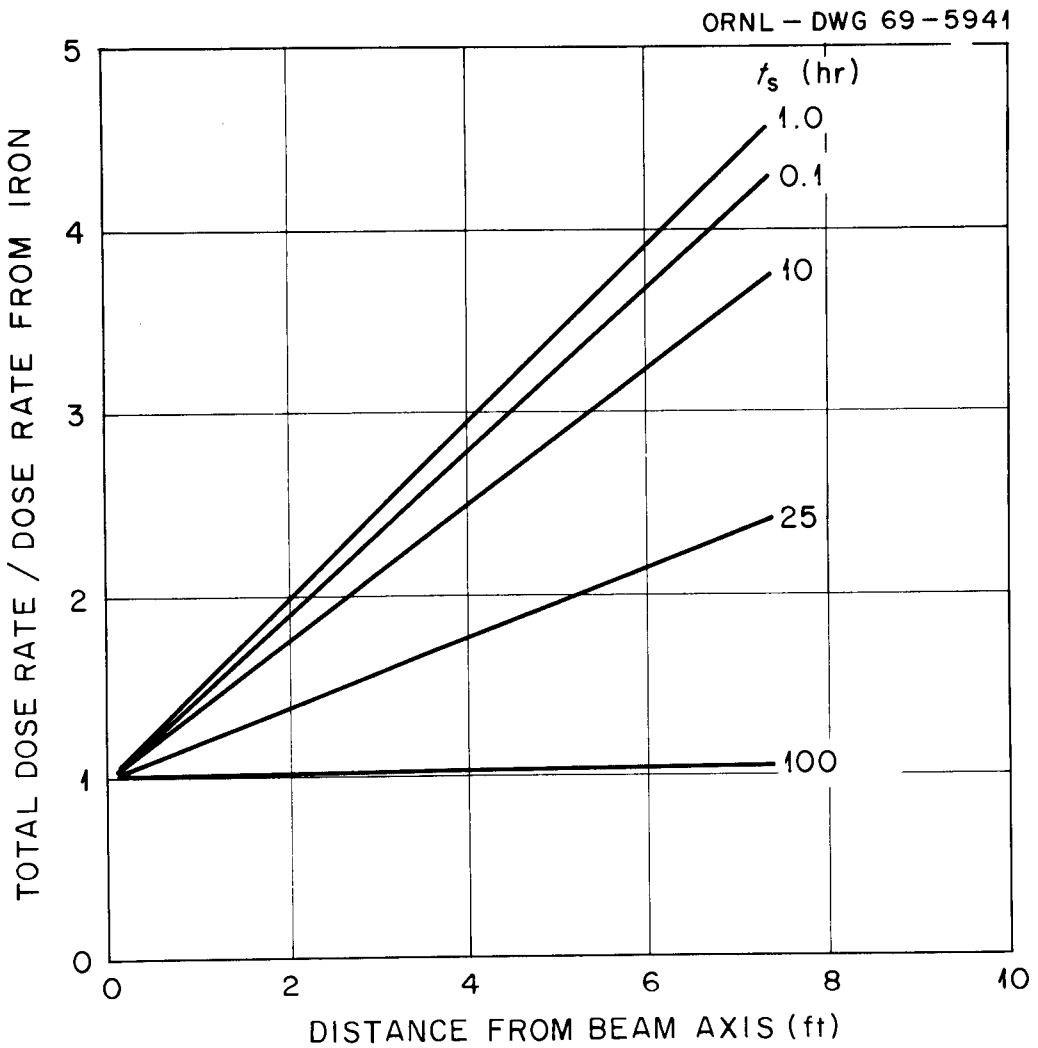

Fig. 8. Ratio of Total Photon Dose Rate to Photon Dose Rate From Iron Inside the Tunnel for Various Shutdown Times.

midway between the iron and concrete would be only a factor of ~ 2.5, with essentially no reduction near the iron.

APPENDIX A

The cross sections used to determine the ^{24}Na production from the constituents of the concrete are given in Figs. A1-A3. The broken lines shown in the figures represent extrapolations or interpolations. The $^{24}Na(n,\gamma)^{23}Na$ cross section, which was taken from Ref. 8, is not shown since it is rather well known and is essentially inversely proportional to the neutron velocity.

The cross section for producing ^{24}Na from ^{40}Ca was calculated using the empirical formula of Rudstam.[7*] This cross-section formula does not take into account the type of particle initiating the interaction; therefore, the cross section shown in Fig. A1 was used for all particles (neutrons, protons, and charged pions).

To obtain the cross section for ^{24}Na production from ^{28}Si, the constant cross section predicted by the Rudstam formula for energies above $\gtrsim$ 2 GeV was extrapolated through the experimental points at lower energies down to the threshold energy (for neutrons) of $\sim$ 40 MeV. The experimental data are for incident protons and were taken from the compilation by Bertini *et al.*[9] The same cross section was used for all particles.

For ^{24}Na production from ^{27}Al, the experimental data for $^{27}Al(n,\alpha)^{24}Na$ reported by Butler and Santry[10] for neutrons < 20 MeV and the experimental data for protons reported by Cumming[11] were used. To obtain the neutron cross section > 20 MeV, extrapolation was made through the value at 50 MeV available from the intranuclear-cascade calculations of Bertini[6] to join

*In the Rudstam paper several different functional forms are considered for the cross section formula. The formula used here is the one designated as CDMD by Rudstam.

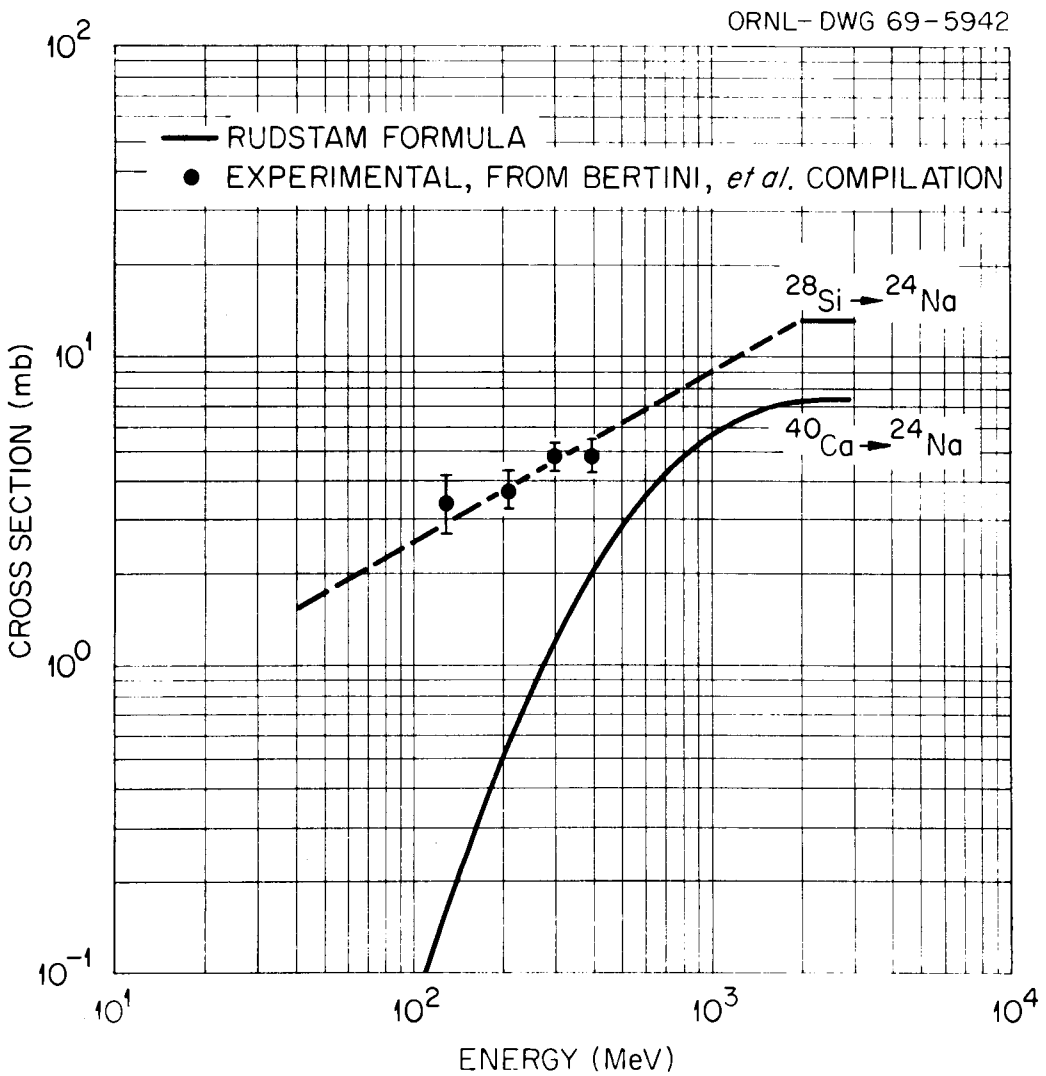

Fig. A1. Cross Sections for Producing ^{24}Na from ^{28}Si and ^{40}Ca.

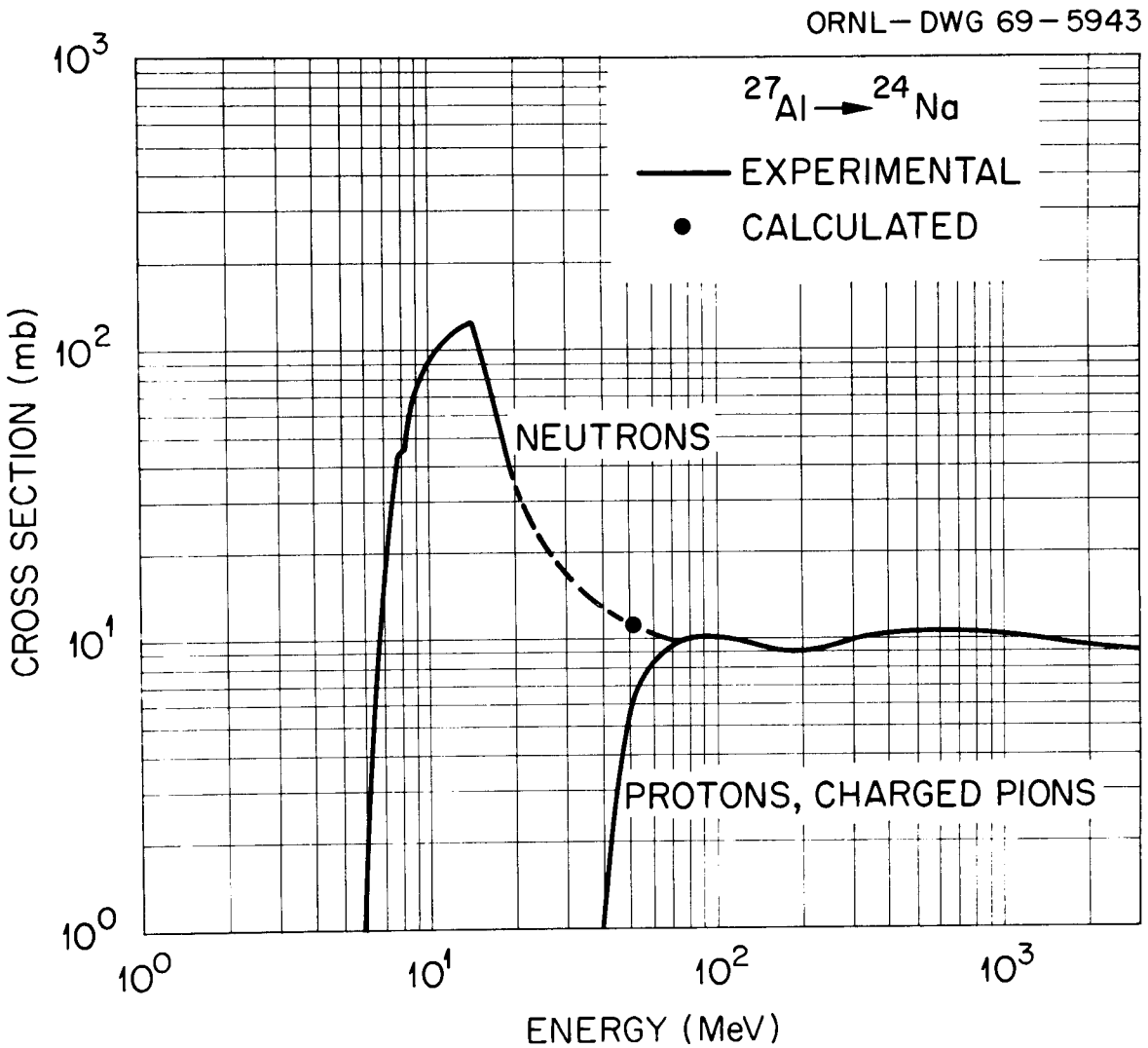

Fig. A2. Cross Section for Producing ^{24}Na from ^{27}Al.

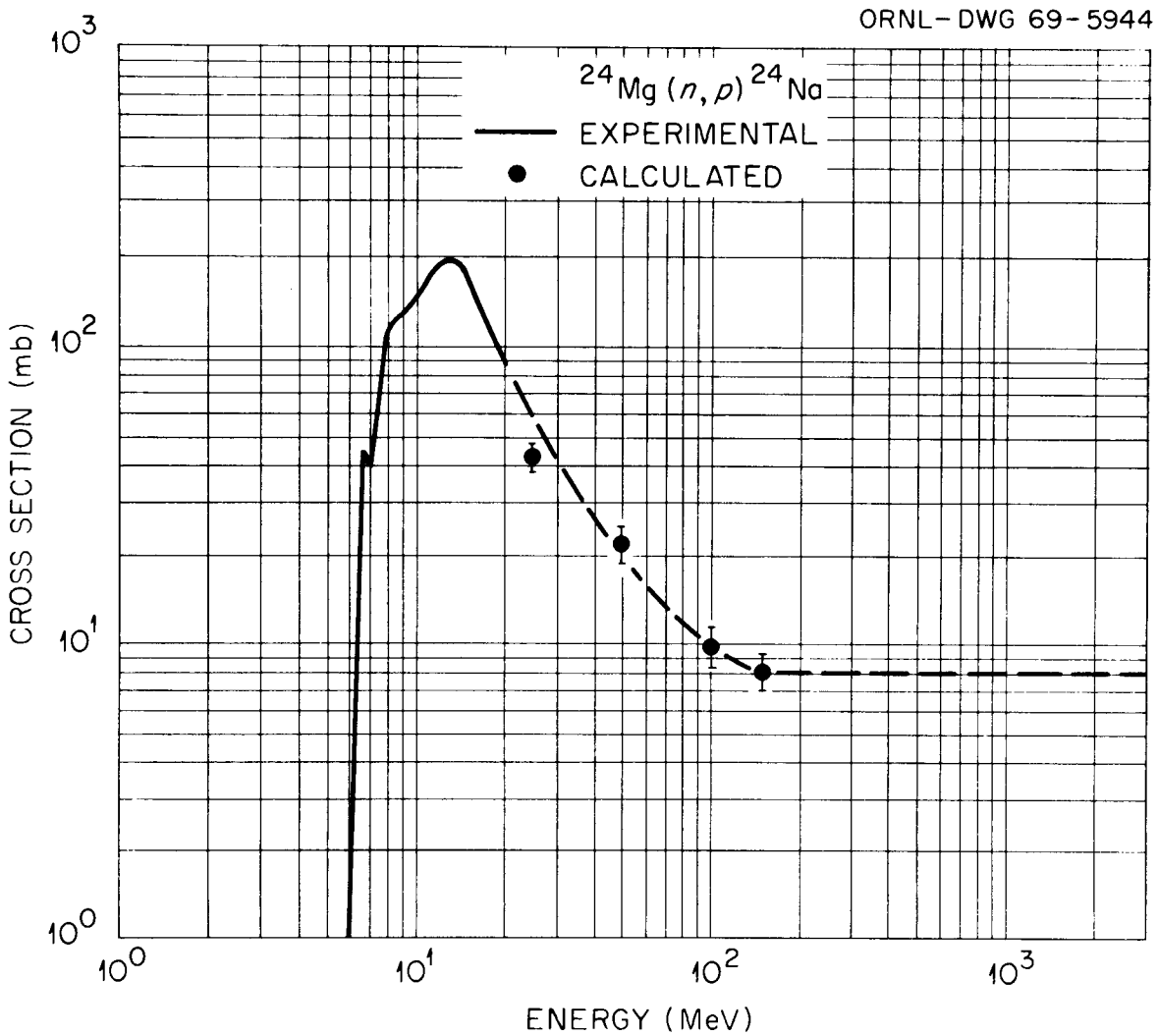

Fig. A3. $^{24}Mg(n,p)^{24}Na$ Cross Section.

with the proton cross section at 80 MeV, and above 80 MeV the neutron cross section was taken to be the same as that for protons. The charged-pion cross sections at all energies were assumed to be the same as for protons.

For the $^{24}Mg(n,p)^{24}Na$ cross section, the experimental data reported by Butler and Santry[10] for neutrons < 20 MeV were used. Between 20 and 150 MeV, extrapolation was made through cross sections obtained using the Bertini intranuclear-cascade code.[12] Above 150 MeV, the cross section was assumed constant and equal to the value at 150 MeV.

APPENDIX B

In this appendix it will be shown that the omnidirectional flux at all points inside a cylindrical void due to an isotropic flux of uniform intensity on the surface of the void is constant and equal to the flux at the surface. Consider the flux $d\phi$ produced in a spherical volume dV with cross-sectional area dA located at $\vec{r}$ due to particles emitted by an element of area dA_s on the surface of the void (see Fig. B1). Then $d\phi$ is the number of particles emitted by $dA_s = Rd\theta dz$ in the direction of dV divided by the cross-sectional area of dV; that is,

$$d\phi = \frac{\phi_o}{4\pi} \vec{\Omega}\cdot\vec{n}\ d\vec{\Omega}/dA \quad ,$$

where ϕ_o is the flux at R, $\vec{\Omega} = \vec{D}/D$, $\vec{n} = -\vec{R}/R$, and $d\vec{\Omega} = dA/D^2$. From the geometry indicated in Fig. B1,

$$-\vec{D} = -\vec{r} + \vec{k}z + \vec{R} \ ,$$

$$\vec{r} = \vec{i}r \ ,$$

and

$$\vec{R} = \vec{i}\ R\cos\theta + \vec{j}\ R\sin\theta \quad ,$$

where $\vec{i}$, $\vec{j}$, and $\vec{k}$ are unit vectors along the x, y, and z axes, respectively. Therefore,

$$\vec{\Omega}\cdot\vec{n} = \frac{R - r\cos\theta}{D} \quad ,$$

and

$$d\phi = \frac{\phi_o}{4\pi} \frac{R(R - r\cos\theta)}{D^3} d\theta dz \quad .$$

ORNL-DWG 69-6542

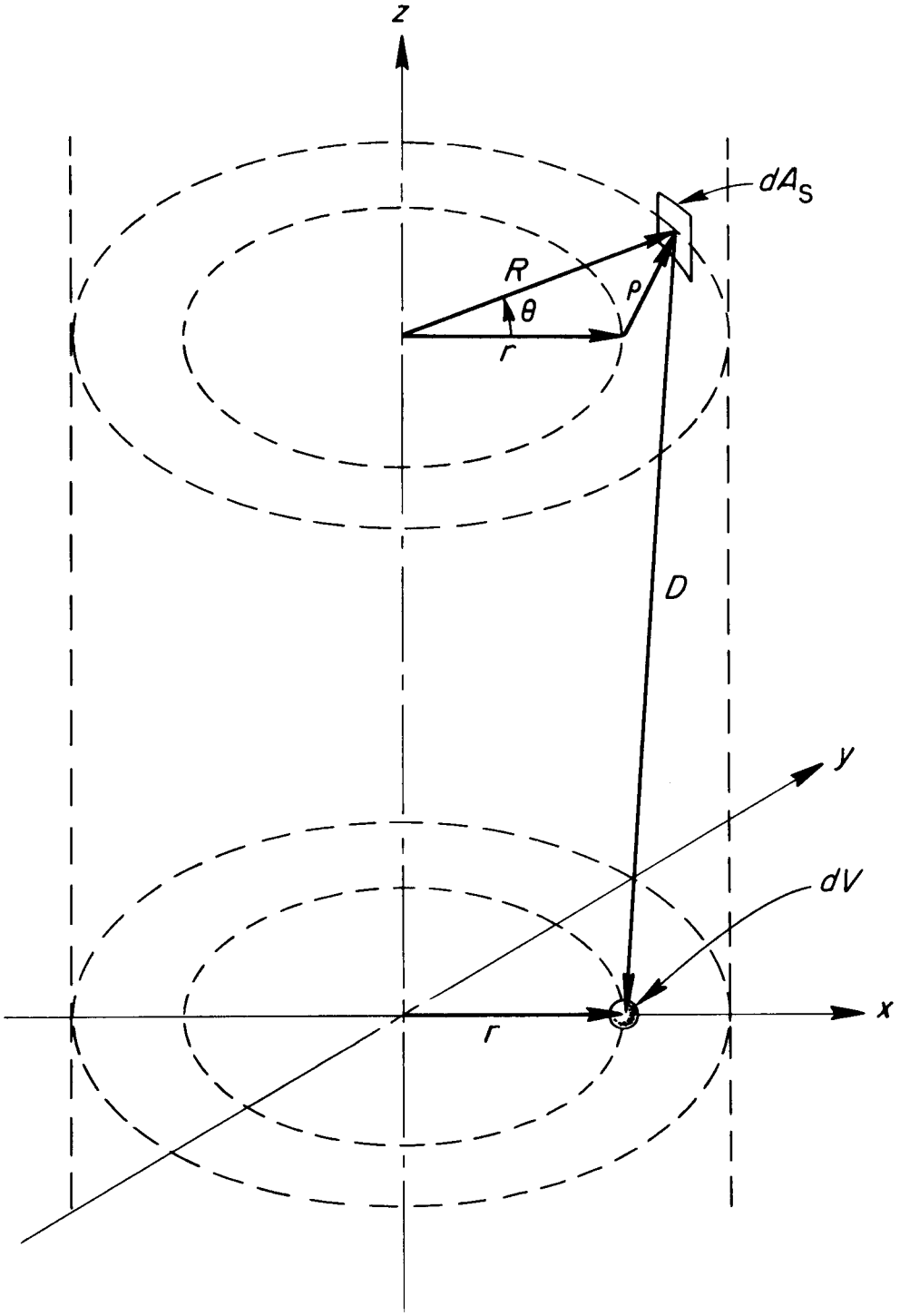

Fig. B1. Definition of Geometry Variables.

Changing variables from z to D using the relation

$$D^2 = z^2 + \rho^2$$

gives

$$\phi = \frac{\phi_o}{2\pi} \int_o^{\pi} R(R - r\cos\theta)\, d\theta \int_{\rho}^{\infty} \frac{dD}{D^2\sqrt{D^2 - \rho^2}} \quad .$$

Both the D and θ integrals can be written in forms which can be found in most standard tables of integrals. The D integral yields $1/\rho^2$. Changing the ρ variable to θ using

$$\rho^2 = R^2 + r^2 - 2R\, r\cos\theta$$

gives

$$\phi = \frac{\phi_o}{\pi} \int_o^{\pi} \frac{R^2 - R\, r\cos\theta}{R^2 + r^2 - 2R\, r\cos\theta}\, d\theta$$

$$= \phi_o \quad .$$

Since ϕ is evaluated at an arbitrary point inside the void, the flux at any point inside the void is the same as the flux at the surface of the void.

ACKNOWLEDGMENT

It is a pleasure to thank Dr. R. G. Alsmiller, Jr. of the Oak Ridge National Laboratory for his many helpful suggestions throughout the course of this work.

FOOTNOTES

a. Research sponsored by the U. S. Atomic Energy Commission under contract with Union Carbide Corporation.

b. At the present time, it is not possible to perform detailed calculations of the residual photon dose rate for beam energies $\gtrsim$ 3 GeV by using the same method of calculation as used here for a 3-GeV beam because of the lack of data concerning such high-energy nuclear interactions. However, the results from a detailed calculation for a 3-GeV beam and a very approximate calculation for a 200-GeV beam presented in paper 1 suggest that extension of the 3-GeV results to higher energies by using a scaling factor proportional to the beam energy is not totally unreasonable.

c. The source-geometry configuration was chosen to aid in the design of the proton accelerator under construction at the National Accelerator Laboratory, Batavia, Illinois, and the concrete composition was supplied by Dr. Miguel Awschalom of that facility.

d. Both ^{34}Cl and ^{38}K can be produced in two isomeric states with half-lives for the ground and metastable states of 7.71 minutes and 0.95 seconds for ^{38}K and 1.56 seconds and 31.99 minutes for ^{34}Cl, respectively. The calculated production rate includes both isomers, and the relative contribution of each cannot be distinguished. It was assumed that all ^{34}Cl is produced in the metastable state and all ^{38}K is produced in the ground state. However, as will be shown later, these radionuclides do not contribute significantly to the total photon dose rate; thus, this assumption is of little consequence.

e. Results in this paper are given for only an infinite irradiation time, that is, for an irradiation time of sufficient duration such that all radionuclides have reached saturation activity. Results for other irradiation times can easily be constructed using the results presented here and in paper 1 and the methods discussed in paper 1.

f. The photons which escape from the iron and are reflected by the concrete have been ignored since the dose albedo of concrete at the photon energies of interest here ($\sim$ 1 MeV) is $\gtrsim$ 10%.[13]

g. The interaction of the photons escaping from the concrete with the iron has been neglected since the radius of the iron (0.168 ft) is small compared to the radius of the tunnel wall (7.34 ft).

h. Note that since the dose rate from the iron varies as c/r and the dose rate from the concrete is constant, say c', where r is the distance from the beam axis and c and c' are constant for given shutdown and irradiation times, the ratio of the total dose rate to the dose rate from the iron varies as 1 + c'r/c inside the tunnel.

REFERENCES

1. T. W. ARMSTRONG and R. G. ALSMILLER, Jr., "Calculation of the Residual Photon Dose Rate Around High-Energy Proton Accelerators," Nucl. Sci. Eng., in press.
2. W. A. COLEMAN and R. G. ALSMILLER, Jr., "Thermal-Neutron Flux Generation by High-Energy Protons," Nucl. Sci. Eng. 34, 108 (1968); see also ORNL-TM-2206, Oak Ridge National Laboratory (1968).
3. D. C. IRVING *et al.*, "05R, A General Purpose Monte Carlo Neutron Transport Code," ORNL-3622, Oak Ridge National Laboratory (1965).
4. D. K. TRUBEY and M. B. EMMETT, "OGRE-G, An OGRE System Monte Carlo Code for the Calculation of Gamma-Ray Dose Rate at Arbitrary Points in an Arbitrary Geometry," ORNL-TM-1212, Oak Ridge National Laboratory (1966).
5. H. C. CLAIBORNE and D. K. TRUBEY, "Gamma-Ray Dose Rates in a Slab Phantom," ORNL-TM-2574, Oak Ridge National Laboratory (1969).
6. H. W. BERTINI, "Results from Low-Energy Intranuclear-Cascade Calculations," ORNL-TM-1225 (1965).
7. S. G. RUDSTAM, "Systematics of Spallation Yields," Z. Naturforschg., 21a, 1027 (1966).
8. E. S. TROUBETZKOY *et al.*, "Fast Neutron Cross Sections of Manganese, Calcium, Sulfur, and Sodium," NDA-2133-4, Nuclear Development Corp. of America (1960).
9. H. W. BERTINI *et al.*, "Literature Survey of Radiochemical Cross-Section Data Below 425 MeV," ORNL-3884, Oak Ridge National Laboratory (1966).

10. J. P. BUTLER and D. C. SANTRY, "Excitation Curves for the Reactions $Al^{27}(n,\alpha)Na^{24}$ and $Mg^{24}(n,p)Na^{24}$," Can. J. Phys., 41, 372 (1963).

11. J. B. CUMMING, "Monitor Reactions for High Energy Proton Beams," Ann. Rev. Nucl. Sci., 13, 261 (1963).

12. T. A. GABRIEL, Oak Ridge National Laboratory, unpublished data, 1969.

13. Engineering Compendium on Radiation Shielding, Vol. I, R. G. Jaeger, ed.-in-chief, Springer-Verlag, New York (1968).

HIGH-ENERGY ACCELERATOR DISTRIBUTION LIST

Argonne National Laboratory, Library Services Department, 302-CE125, 9700 South Cass Avenue, Argonne, Ill. 60439

Armed Forces Radiobiology Research Institute, Defense Atomic Support Agency, National Naval Medical Center, Bethesda, Md. 20014

Army Materials and Mechanics Research Center, ATTN: Technical Information Branch, Watertown, Mass. 02172

Louis Avrami, Radiation Effects and Support Branch, Explosives Laboratory, SMUPA-VE3, Bldg. 407, Picatinny Arsenal, Dover, New Jersey 07801

Miguel Awschalom, National Accelerator Laboratory, P. O. Box 500, Batavia, Ill. 60510

V. S. Barashenkov, Laboratory of Theoretical Physics, Joint Institute for Nuclear Research, Head Post Office P. O. Box 79, Moscow, USSR

Sherwin M. Beck, NASA/Langley Research Center, Mail Stop 400, Hampton, Va. 23365

J. R. Beyster, Scientific Applications, P. O. Box 2351, La Jolla, Cal. 92037

F. L. Bouquet, Dept. 72-71, B-6, Lockheed California Co., Burbank, Cal. 91503

S. Bresticker, Space Adv. Systems, Pl. 5, Grumman Aircraft, Bethpage, New York 11714

Brookhaven National Laboratory, ATTN: Research Library, Upton, N. Y. 11973

Walter R. Burrus, Tennecomp, Inc., P. O. Box J, Oak Ridge, Tenn. 37830

Richard L. Childers, Physics Department, University of South Carolina, Columbia, South Carolina 25205

Chief Nuclear Engineer, The Kuljian Corporation, 1200 North Broad Street, Philadelphia, Pa. 19121

Maj Anthony J. Chiota, HQ AFSC (SCTSW), Andrews AFB, Washington, D. C. 20331

Wayne A. Coleman, 6615B Jacob Street, Edgewood, Maryland 21040

Consultant, Nuclear Medicine, Office of the Surgeon General, Washington, D. C. 20315

Frederick P. Cowan, Head, Health Physics Division, Brookhaven National Laboratory, Upton, New York 11973

Richard B. Curtis, Office of Research and Advanced Studies, Indiana University, Bloomington, Ind. 47401

Stanley B. Curtis, Bldg. 29, Room 213, Lawrence Radiation Laboratory, Berkeley, Calif. 94720

J. De Juren, 3401 West Broadway Avenue, Hawthorne, Calif. 90250

Herbert DeStaebler, SLAC, Stanford University, Stanford, Calif. 94305

Director, Defense Atomic Support Agency, ATTN: APTL, Washington, D. C. 20305

Director, Defense Atomic Support Agency, ATTN: RARP, Washington, D. C. 20305

Israel Dostrovsky, Weizmann Institute of Science, Rehovath, Israel

R. D. Edge, Physics Department, University of South Carolina, Columbia, South Carolina 29208

T. Fuse, Ship Research Institute, Shinkaway, Mitaka, Tokyo, Japan

Russell R. Galasso, Headquarters, USA Test and Evaluation Command, Aberdeen Proving Ground, Md. 21005

General Dynamics/Fort Worth, ATTN: B. S. Fain and K. G. Brown, P. O. Box 748, Fort Worth, Texas 76101

Frederick Gordon, Jr., NASA/Goddard Space Flight Center, Code 716A, Greenbelt, Md. 20771

Raymond M. Hansen, Mail Stop 235, NASA/Langley Research Center, Hampton, Va. 23365

Herbert D. Hendricks, NASA/Langley Research Center, Mail Stop 499, Hampton, Va. 23365

W. N. Hess, Director, Division of Science and Applications, Manned Spacecraft Center, Houston, Texas

Doris M. High, Librarian, Commanding Officer, U. S. Army Nuclear Defense Laboratory, Bldg. 5695, ATTN: Library, Edgewood Arsenal, Md. 21010

Charles W. Hill, Dept. 73-69, Zone 174, Lockheed-Georgia Company, Marietta, Ga. 30060

John R. Hoffman, Kaman Nuclear, 1700 Garden of the Gods Road, Colorado Springs, Colorado 80907

George R. Holeman, Health Physicist, Yale University, Health Physics Division, 1136 Kline Biology Tower, 219 Prospect Street, New Haven, Conn. 06520

Holmes and Narver, Inc., 828 South Figueroa St., Los Angeles, Calif. 90017

H. E. Hungerford, 101 Michael Golden Laboratory, Purdue University, Lafayette, Ind. 47907

T. Inada, National Institute of Radiological Sciences, Anagawa, Chibashi, Japan

Harvey I. Israel, H-DO, Los Alamos Scientific Laboratory, P. O. Box 1663, Los Alamos, New Mexico 87544

Philippe Tardy-Joubert, S.P.R., Centre d'Etudes Nucleaires de Saclay, B. P. 2, 91-Gif-Sur-Yvette, France

J. Warren Keller, NASA Headquarters, Code RV-1, Washington, D. C. 20546

D. Aliaga-Kelly, Nuclear Enterprises Ltd., Sighthill, Edinburgh 11, Scotland

E. M. Kinderman, Radiation Physics Division, Stanford Research Institute, Menlo Park, Calif. 94025

B. Larsson, The Gustaf Werner Institute, University of Uppsala, Box 531, 75121 Uppsala, Sweden

Lawrence Radiation Laboratory, Technical Information Department, P. O. Box 808, Livermore, Calif. 94550

Martin Leimdorfer, Industri-Matematik AB, De Geersgatan 8, 11529 Stockholm, Sweden

V. Lebedev, Institute of High Energy Physics, Serpukhov, Moscow Region, USSR

Library, Cambridge Electron Accelerator, Harvard University, 42 Oxford Street, Cambridge, Mass. 02138

Library, Kaman Nuclear, 1700 Garden of the Gods Road, Colorado Springs, Colorado 80907

The Librarian, Saha Institute of Nuclear Physics Library, 92, Acharya Prafully Chandra Road, Calcutta 9, India

Lockheed Missiles and Space Co., Technical Information Center, 3251 Hanover Street, Palo Alto, Calif. 94304

A. Manning, Department of Physics, Valparaiso University, Valparaiso, Ind. 46383

James E. McLaughlin, Director, Radiation Physics, U. S. Atomic Energy Commission, 376 Hudson Street, New York, N. Y. 10014

Albert Metzger, Jet Propulsion Laboratory, 4800 Oak Grove Drive, Pasadena, Calif. 91103

J. M. Miller, Department of Chemistry, Columbia University, New York, N. Y. 10027

John C. Mitchell, USAF School of Aerospace Medicine, SAM Box 4376, Brooks AFB, Texas 78235

Phillip S. Mittelman, 180 South Broadway, White Plains, N. Y. 10605

National Aeronautics and Space Administration, Langley Research Center, ATTN: Dr. Jag J. Singh, MS 235, Langley Station, Hampton, Va. 23365

NASA Scientific and Technical Information Facility, ATTN: Acquisitions Branch, P. O. Box 33, College Park, Md. 20740

W. R. Nelson, Stanford Linear Accelerator Center, P. O. Box 4349, Stanford University, Stanford, Calif.

Keran O'Brien, U. S. Atomic Energy Commission, Health and Safety Laboratory, 376 Hudson Street, New York, N. Y. 10014

Radiation Effects Information Center, Battelle Memorial Institute, Columbus Laboratories, 505 King Avenue, Columbus, Ohio 43201

J. Ranft, Science Research Council, Rutherford High Energy Laboratory, Bldg. R25, Chilton, Didcot, Berkshire, England

Arthur Reetz, Jr., NASA Headquarters, Code RV-1, Washington, D. C. 20546

David L. Rigotti, U. S. Army Nuclear Defense Laboratory, Edgewood AArsenal, Md. 21010

Robert B. Seale, Department of Nuclear Engineering, University of Arizona, Tucson, Arizona 85721

W. E. Selph, LINAC, Gulf General Atomic, Inc., P. O. Box 608, San Diego, Calif. 92112

K. Shure, Westinghouse Electric Corp., Bettis Atomic Power Laboratory, P. O. Box 79, West Mifflin, Pa. 15122

Robert T. Seigel, Director, Space Radiation Effects Laboratory, Operated by College of William and Mary, 11970 Jefferson Avenue, Newport News, Va. 23606

Charles A. Sondhaus, Associate Professor, Department of Radiological Sciences, College of Medicine, University of California, Irvine, Calif. 92664

Stanford Linear Accelerator Center, ATTN: Library, P. O. Box 4349, Stanford, Calif. 94305

G. R. Stevenson, Radiation Protection Group, R20, Rutherford High Energy Laboratory, Chilton, Didcot, Berkshire, England

J. A. Swartout, Union Carbide Corporation, 270 Park Avenue, New York, N. Y. 10017

Maj Eugene J. Swick, HQ SAMSO/SMTS-1, Norton AFB, Calif. 92409

Eizo Tajima, Rikkyo University, Nishi-Ikebukuro, Toshimaku, Tokyo, Japan

R. F. Taschek, Los Alamos Scientific Laboratory, Los Alamos, N. M. 87544

R. Tesch, DESY, Hamburg, Notkesteig 1, Germany

Ralph H. Thomas, Health Physics, 67 Encina Hall, Stanford University, Stanford, Calif. 94305

W. Turchinetz, R26-411, Massachusetts Institute of Technology, Cambridge, Mass. 02139

Roger Wallace, Bldg. 72, Lawrence Radiation Laboratory, Berkeley, Cal. 94720

M. B. Wells, Radiation Research Associates, Inc., 3550 Hulen Street, Fort Worth, Texas 76107

Robert V. Wheeler, R. S. Landauer, Jr., and Co., Glenwood Science Park, Glenwood, Ill. 60425

Ralph Wiley, Mail Zone Y-128, General Dynamics, Fort Worth, Texas 76101

William R. Yucker, 3250 Greenfield Avenue, Los Angeles, Calif. 90034

Internal Distribution

1-3. L. S. Abbott
4. F. S. Alsmiller
5-264. R. G. Alsmiller, Jr.
265-289. T. W. Armstrong
290-294. J. Barish
295. H. W. Bertini
296. C. E. Clifford
297. T. A. Gabriel
298. M. P. Guthrie
299. D. C. Irving
300. D. T. King
301. T. A. Love
302-303. F. C. Maienschein
304. H. S. Moran
305. R. W. Peelle
306. R. T. Santoro
307. D. Sundberg
308. D. K. Trubey
309. J. W. Wachter
310. J. W. Webster
311. W. Zobel
312. E. R. Cohen (consultant)
313. B. C. Diven (consultant)
314-315. Central Research Library
316. ORNL Y-12 Technical Library Document Reference Section
317-318. Laboratory Records Department
319. Laboratory Records ORNL RC
320. ORNL Patent Office

External Distribution

321. P. B. Hemmig, Division of Reactor Development & Technology, U. S. Atomic Energy Commission, Washington, D. C.
322. W. H. Hannum, Division of Reactor Development & Technology, U. S. Atomic Energy Commission, Washington, D. C.
323. Herbert Goldstein, 287A Mudd Building, Columbia University, New York.
324. Kermit Laughon, AEC Site Representative
325-410. Given AEC High-Energy Accelerator Shielding Distribution as shown on preceding pages.
411-425. Division of Technical Information Extension (DTIE).
426. Laboratory and University Division (ORO).